



An Agomir of miR-144-3p Accelerates Plaque Formation through Impairing Reverse Cholesterol Transport and Promoting Pro-Inflammatory Cytokine Production

Yan-Wei Hu^{1*}, Ya-Rong Hu^{1*}, Jia-Yi Zhao¹, Shu-Fen Li¹, Xin Ma², Shao-Guo Wu¹, Jing-Bo Lu³, Yu-Rong Qiu¹, Yan-Hua Sha¹, Yan-Chao Wang¹, Ji-Juan Gao¹, Lei Zheng^{1*}, Qian Wang^{1*}

1 Laboratory Medicine Center, Nanfang Hospital, Southern Medical University, Guangzhou, Guangdong, China, **2** Department of Anesthesiology, Nanfang Hospital, Southern Medical University, Guangzhou, Guangdong, China, **3** Department of Vascular Surgery, Nanfang Hospital, Southern Medical University, Guangzhou, Guangdong, China

Abstract

Aims: ATP-binding cassette transporter A1 (ABCA1) mediates the efflux of cholesterol and phospholipids to lipid-poor apolipoproteins, which then form nascent HDL, a key step in the mechanism of reverse cholesterol transport (RCT). While a series of microRNAs (miRNAs) have been identified as potent post-transcriptional regulators of lipid metabolism, their effects on ABCA1 function and associated mechanisms remain unclear.

Methods and Results: ABCA1 was identified as a potential target of miR-144-3p, based on the results of bioinformatic analysis and the luciferase reporter assay, and downregulated after transfection of cells with miR-144-3p mimics, as observed with real-time PCR and western blot. Moreover, miR-144-3p mimics (agomir) enhanced the expression of inflammatory factors, including IL-1 β , IL-6 and TNF- α , *in vivo* and *in vitro*, inhibited cholesterol efflux in THP-1 macrophage-derived foam cells, decreased HDL-C circulation and impaired RCT *in vivo*, resulting in accelerated pathological progression of atherosclerosis in apoE^{-/-} mice. Clinical studies additionally revealed a positive correlation of circulating miR-144-3p with serum CK, CK-MB, LDH and AST in subjects with AMI.

Conclusions: Our findings clearly indicate that miR-144-3p is essential for the regulation of cholesterol homeostasis and inflammatory reactions, supporting its utility as a potential therapeutic target of atherosclerosis and a promising diagnostic biomarker of AMI.

Citation: Hu Y-W, Hu Y-R, Zhao J-Y, Li S-F, Ma X, et al. (2014) An Agomir of miR-144-3p Accelerates Plaque Formation through Impairing Reverse Cholesterol Transport and Promoting Pro-Inflammatory Cytokine Production. PLoS ONE 9(4): e94997. doi:10.1371/journal.pone.0094997

Editor: Olivier Kocher, Harvard Medical School, United States of America

Received January 22, 2014; **Accepted** March 20, 2014; **Published** April 14, 2014

Copyright: © 2014 Hu et al. This is an open-access article distributed under the terms of the Creative Commons Attribution License, which permits unrestricted use, distribution, and reproduction in any medium, provided the original author and source are credited.

Funding: The authors gratefully acknowledge financial support from the National Natural Sciences Foundation of China (81301489 and 81271905), Guangdong Provincial Natural Sciences Foundation of China (S2012020010920), and the President Foundation of Nanfang Hospital, Southern Medical University. The funders had no role in study design, data collection and analysis, decision to publish, or preparation of the manuscript.

Competing Interests: The authors have declared that no competing interests exist.

* E-mail: nfyywangqian@163.com (QW); nfyyz@163.com (LZ)

• These authors contributed equally to this work.

Introduction

Atherosclerotic cardiovascular disease remains the leading cause of morbidity and mortality worldwide. Epidemiological studies have revealed that blood lipid abnormality is a key risk factor. High-density lipoprotein cholesterol (HDL-C) level is inversely correlated with rates of coronary events, and therefore considered cardioprotective [1–2]. Recent advances have established a fundamental role for inflammation in mediating all stages of this disease from initiation through progression of atherosclerosis [3]. These findings reveal new insights into the significant associations between risk factors and the mechanisms of atherogenesis.

Several ATP-binding cassette (ABC) transporters, such as ABCA1 and ABCG5, have been shown to play important roles in the regulation of cell cholesterol homeostasis [4]. In extrahepatic cells and tissues, ABCA1 mediates the efflux of cholesterol and phospholipids to lipid-poor apolipoproteins, which subse-

quently form nascent HDL, a key step in the mechanism of reverse cholesterol transport (RCT). Deficiency in ABCA1 is reported to lead to a dramatic reduction in plasma HDL levels. Mutations in the ABCA1 gene result in Tangier disease, a rare inherited disorder characterized by severe reduction in the amount of HDL and increased risk of atherosclerosis [5,6].

In addition to classic transcriptional regulation of cholesterol metabolism, members of a class of microRNAs (miRNAs) have been identified as potent post-transcriptional regulators of lipid metabolism. Recently, miRNA-33a and b (miR-33a/b) were identified as key regulators of metabolic programs, including cholesterol and fatty acid homeostasis. These intronic miRNAs are embedded in the genes for sterol response element-binding proteins, SREBF2 and SREBF1, which code for transcription factors that modulate cholesterol and fatty acid synthesis [7,8]. In addition to miR-33a/b, miR-122, miR-370, miR-335, miR-378/378*, miR-27 and miR-125a-5p have been implicated in

regulating cholesterol homeostasis, fatty acid metabolism and lipogenesis [9].

Data from the current study showed that miR-144-3p mimics (agomir) suppress the expression of ABCA1 and enhance inflammatory factors, both *in vitro* and *in vivo*, inhibit cholesterol efflux in THP-1 macrophage-derived foam cells and impair RCT in apoE^{-/-} mice fed a high-fat diet (HFD), leading to accelerated pathological progression of atherosclerosis in experimental mice. Clinical studies additionally revealed a significant association between circulating miR-144-3p and acute myocardial infarction (AMI). These findings collectively suggest that miR-144-3p may be effectively used as a potential therapeutic target of atherosclerosis and promising diagnostic biomarker of AMI.

Materials and Methods

Our study was conformed with the Declaration of Helsinki and approved by the Institutional Review Board of Nanfang Hospital, Southern Medical University (Guangzhou, China) and written informed consent was obtained from all subjects.

Animals

This investigation conforms with the Guide for the Care and Use of Laboratory Animals published by the US National Institutes of Health (NIH Publication No. 85–23, revised 1996), and was approved by the Animal Experimental Committee at Nanfang Hospital. Male six-week-old apoE^{-/-} mice with a C57BL/6 background were purchased from Vital River Laboratory Animal Technology Co, Ltd (Beijing, China). Mice were randomized into two groups (Control and miR-144-3p agomir, n = 20/group) and injected via the tail vein with either a scrambled miRNA agomir (GuangZhou RiboBio. Co.) or miRNA analog (agomir) of mir-144-3p (GuangZhou RiboBio. Co.) at a dose of 20 mg/kg/day in 0.2 ml saline twice a week. Five animals were housed per cage at 25°C under a 12-h light/dark cycle. The mice were fed a high-fat diet (HFD) for a period of 12 weeks. The diet is a commercially prepared mouse food supplemented with 21% (wt/wt) butterfat, 0.15% (wt/wt) cholesterol, and 19.5% (wt/wt) casein (Beijing Keao Xieli Feed Co.LTD., Beijing). At week 12, mice were anesthetized, and 1 mL of blood collected via cardiac puncture before sacrifice via cervical dislocation. Tissues were collected for further analysis.

Cell Culture

Human monocytic THP-1 cells were obtained from American Type Culture Collection (ATCC, Manassas, VA, USA). THP-1 cells were maintained in Roswell Park Memorial Institute (RPMI) 1640 medium containing 10% fetal calf serum (FCS) and differentiated for 72 h with 100 nM phorbol 12-myristate 13-acetate (PMA). Macrophages were transformed into foam cells by incubation in the presence or absence of 50 µg/mL ox-LDL in serum-free RPMI 1640 containing 0.3% BSA for 48 h. All cells were incubated at 37°C in an atmosphere of 5% CO₂, seeded in 6- or 12-well plates or 60-mm dishes, and grown to 60–80% confluence before use.

Isolation and Culture of Primary Human Macrophages

Peripheral blood mononuclear cells were prepared from forearm venous blood of healthy volunteers using Biocoll density gradient centrifugation, as described previously [10]. Monocytes (CD14+) were selected using paramagnetic beads according to the manufacturer's instructions (Miltenyi Biotech, Bergisch Gladbach, Germany), cultured in RPMI 1640 containing 10% homologous or AB serum on poly-L-lysine-coated 6-well plates at a density of 2

million cells per well, and incubated at 37°C under 5% CO₂. All cell culture experiments were performed after 8 days of differentiation. For cells in different experimental settings, supplemented RPMI 1640 was replaced with serum-free RPMI 1640. Macrophage differentiation of primary human monocytes was monitored morphologically via light microscopy and fluorescence-activated cell sorting (FACS) analysis using a monoclonal antibody specific for CD163.

Transfection of miRNA Mimics

THP-1 macrophages were transfected with 50 nM miRNA mimic (hsa-miR-144-3p, UACAGUAUAGAUGAUGUACU) using Lipofectamine 2000 transfection reagent for 48 h, according to the manufacturer's instructions. All experimental control samples were treated with equal concentrations of a non-targeting control mimic sequence (negative control, UUUGUACUACACAAAAA-GUACUG).

Luciferase Assay

Human ABCA1 cDNA containing putative (wild-type) and mutated target sites for hsa-miR-144-3p was chemically synthesized, and inserted into pMIR-REPORT vector (Ambion, Austin, TX, USA). The pMIR-REPORT beta-galactosidase control vector (Ambion) was used as a reference. For the luciferase assay, 293T cells (human embryonic kidney) were co-transfected with wild-type (pMIR-ABCA1-wt) or mutant (pMIR-ABCA1-mt) reporter vectors and hsa-miR-144-3p mimics, using Lipofectamine 2000 transfection reagent. Luciferase activity was measured at 48 h post-transfection using a dual-luciferase assay kit (Promega, Madison, WI, USA).

RNA Isolation and Real-time Quantitative PCR

Total RNA from tissues or cultured cells was extracted using TRIzol reagent (Invitrogen, Carlsbad, CA, USA), according to the manufacturer's instructions. Total RNA from 200 µL serum was isolated using the miRVana PARIS kit (Ambion, Austin, TX, USA). mir-144-3p was detected with the All-in-One miRNA qPCR Kit (GeneCopoeia, Rockville, MD, USA) in a 20 µL reaction volume, using the manufacturer's protocol. Real-time quantitative PCR (qRT-PCR) was performed on the ABI 7500 Fast system (Applied Biosystems, Foster City, CA, USA). U6 RNA expression was used as the endogenous control for analysis of miR-144-3p from cells and tissues. For serum miR-144-3p analysis, isolation and assay were performed using a series of concentrations of miR-144-3p (synthesized by IDT, Coralville, IA, USA) to generate a standard curve. The absolute amount of miR-144-3p was calculated with software based on sample qRT-PCR numbers and the standard curve, and expressed as pmol/L. mRNA levels were evaluated with qRT-PCR using an ABI 7500 Fast Real Time PCR system with SYBR Green detection chemistry (TaKaRa Bio, Inc., Shiga, Japan). Expression of glyceraldehyde-3-phosphate dehydrogenase was used as the internal control. Quantitative measurements were performed using the ΔΔCt method. All samples were measured in triplicate, and mean values considered for comparative analysis.

Western Blot Analyses

Cells and tissues were harvested and protein extracts prepared using established methods. Extracts were separated using 10% sodium dodecyl sulfate polyacrylamide gel electrophoresis and subjected to western blot using rabbit polyclonal anti-ABCA1 antibodies (Abcam Inc., Cambridge, MA, USA) and rabbit polyclonal anti-β-actin antibody (Santa Cruz Biotechnologies,

Inc., Santa Cruz, CA, USA). Proteins were visualized using the chemiluminescence method (ECL Plus Western Blot Detection System; Amersham Biosciences, Foster City, CA, USA).

Cytokine Assays and Measurement of Serum Biochemical Parameters

Human IL-1 β , IL-6 and TNF- α contents in culture medium (R&D Systems, Minneapolis, MN, USA), serum concentrations of IL-1 β , IL-6 and TNF- α (R&D Systems, Minneapolis, MN, USA), and levels of serum apolipoprotein A1 and apolipoprotein B (Cusabio Biotech Co., Ltd., Wuhan, China) were measured using ELISA according to the manufacturer's instructions. Plasma TC and TG levels were analyzed in an automated analyzer (Beckman AU5400). Lipoproteins were isolated by sequential ultracentrifugation from 60 μ L of plasma at densities (d) of <1.006 g/mL (very-low-density lipoprotein), 1.006≤ d ≤1.063 g/mL (intermediate-density lipoprotein and low-density lipoprotein) and d >1.063 g/mL (high density lipoprotein) in a LE-80K ultracentrifuge (Beckman). Cholesterol in the lipoprotein fractions was determined enzymatically using a colorimetric method (Beckman AU5400).

HPLC Analysis of Cellular Cholesterol Levels

High-performance liquid chromatography (HPLC) analysis was conducted, as described previously [11]. Sterol analyses were performed using a HPLC system (model 2790, controlled with Empower Pro software; Waters Corp., Milford, MA, USA). Absorbance at 216 nm was monitored, and data analyzed with TotalChrom software from PerkinElmer (Waltham, MA, USA).

Cellular Cholesterol Efflux Experiments

THP-1 macrophages were labeled with 0.2 μ Ci/mL [3 H] cholesterol and cholesterol-loaded using 50 μ g/ml oxidized LDL. After 72 h, cells were washed with PBS and incubated overnight in RPMI 1640 containing 0.1% (w/v) BSA to allow equilibration of [3 H] cholesterol in all cellular pools. Equilibrated [3 H] cholesterol-labeled cells were washed with PBS and incubated in 2 mL efflux medium containing RPMI 1640 and 0.1% BSA with 25 μ g/mL of human plasma apoAI or 100 μ g/mL of human plasma HDL for 12 h. A 150 μ L sample of efflux medium was obtained at the designated times and passed through a 0.45- μ m filter to remove floating cells. Monolayers were washed twice with PBS, and cellular lipids extracted with isopropanol. Medium and cell-associated [3 H] cholesterol were measured using liquid scintillation counting. Percent efflux was calculated using the following equation: [total media count/(total cellular count + total media count)] × 100%.

In Vivo RCT Assay

Bone marrow-derived macrophages were prepared from C57BL/6 mice, as described previously [12]. Bone marrow was isolated, and cells were plated overnight in DMEM supplemented with 10% FBS and 15% L-929 conditioned medium. Non-adherent cells were removed and cultured for an additional 6 days to allow for macrophage differentiation. For RCT assays, bone marrow-derived macrophages (BMDMs) were washed twice and incubated with 37.5 μ g/mL of acetylated LDL (Ac-LDL) and 5 μ Ci/mL of [3 H]-cholesterol for 24 h [13]. Cells were resuspended in ice-cold DMEM, and an aliquot (3×10^6 cells) injected subcutaneously into individually housed mice treated with either scrambled miRNA agomir or miRNA analog (agomir) of miR-144-3p for 12 weeks, as described above. Prior to injection, an aliquot of cells was quantified using liquid scintillation counting to measure baseline radioactivity. Blood was obtained via saphenous

vein puncture at 6, 12, and 24 h after BMDM injection and cardiac puncture after 48 h at sacrifice. An aliquot of plasma was used for liquid scintillation counting immediately at each time-point. Feces were collected for 48 h after injection, homogenized in 50% NaOH overnight, and an aliquot used for liquid scintillation counting. At sacrifice, animals were perfused with PBS to remove the blood and then liver samples were collected and incubated with hexane/isopropanol (3:2) for 48 h and dried overnight. Lipids were resolubilized in liquid scintillation fluid, and radioactivity counted. RCT to plasma, liver, and feces was calculated as a percentage of total radioactivity injected at baseline.

En Face Plaque Area

After mice were sacrificed, aortas were excised immediately and fixed in 10% buffered formalin for quantification of the en face plaque areas. Briefly, after adventitial tissue was carefully removed, the aorta was opened longitudinally, stained with Oil Red O (Sigma), and pinned on a blue wax surface. En face images were obtained under a stereomicroscope (SZX12; Olympus, Tokyo, Japan) equipped with a digital camera (Dxm1200, Nikon, Tokyo, Japan) and analyzed using Adobe Photoshop version 7.0 and Scion Image software. The luminal surface area stained with Oil Red O was determined as a percentage [14].

Quantification of Atherosclerosis in the Aortic Sinus

The upper portion of the heart and proximal aorta were obtained, embedded in Optimal Cutting Temperature (OCT) compound (Fisher, Tustin, CA), and stored at -70°C. Serial 10- μ m thick cryosections of aorta, beginning at the aortic root, were collected for a distance of 400 μ m. Sections were stained with Oil Red O. Aortic root atherosclerosis was assessed as the average of three sections, each separated by 100 μ m, beginning at the site of appearance of the coronary artery and valve leaflets. The Oil Red O-positive areas in digitized color images of stained aortic root sections were quantified using Image-Pro Plus image analysis software (Media Cybernetics, Rockville, MD, USA), and data expressed as a percentage of the total section area.

Blood Samples

AMI was diagnosed, based on a combination of several criteria: 1) ischemic symptoms, 2) increased cardiac cTnI level, 3) creatine kinase-MB (CK-MB), 4) pathological Q wave, and 5) ST-segment elevation or depression [15]. In total, 25 healthy volunteers (with normal electrocardiogram and no history of cardiovascular disease) were enrolled in this study. Blood samples of patients with AMI were obtained at 4 h (± 30 min), 8 h (± 30 min), 12 h (± 30 min), 24 h (± 30 min), 48 h (± 30 min), 72 h (± 30 min) and 1 week (± 60 min) after the onset of symptoms. Plasma was isolated via centrifugation and maintained at -80°C until RNA extraction.

Statistical Analysis

Data are expressed as mean values \pm standard deviations (SD). Results were analyzed with one-way ANOVA analysis of variance followed by the Student-Newman-Keuls (SNK) test and the Student's *t*-test using SPSS v13.0 statistical software (SPSS, Inc., Chicago, IL, USA). A two-tailed probability (p) value <0.05 was considered statistically significant.

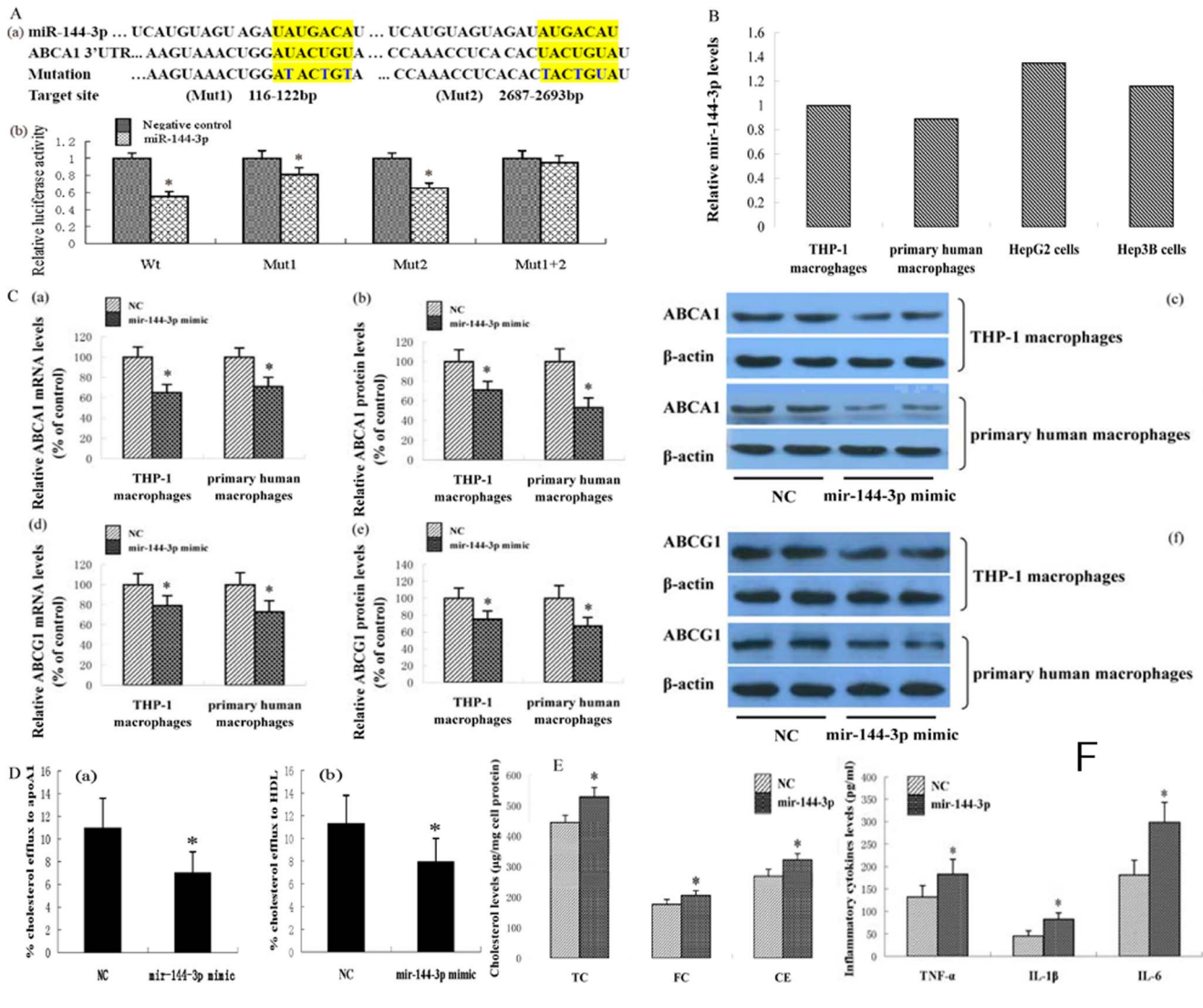


Figure 1. Effects of miR-144-3p on ABCA1 expression, cholesterol homeostasis and inflammation. (A) hsa-miR-144-3p directly targeted the 3'-untranslated region (3'UTR) of ABCA1. (a) Sequence alignment of the human hsa-miR-144-3p mature sequence with the binding sites of human ABCA1 3'UTR. (b) Changes in luciferase activity induced by the hsa-miR-144-3p mimic in binding to ABCA1 3'-UTR ($n=3$; * $p<0.01$ vs. 293T cells transfected with negative control miRNAs). (B) miR-144-3p expression levels in various cells were analyzed by qRT-PCR. (C) THP-1 macrophages and primary macrophages were exposed to 50 μ g/mL of oxidized LDL for 48 h and then treated with 50 nM miRNA mimics, as indicated, for 48 h. ABCA1 mRNA and protein levels were measured using qRT-PCR and western blot analysis, respectively. (D) THP-1 cells were differentiated for 72 h with 100 nM PMA and then macrophages were treated with 50 nM miRNA mimics for 48 h. Then, the cells were labeled with 0.2 μ Ci/mL [3 H] cholesterol and cholesterol-loaded using 50 μ g/ml oxidized LDL. The percentage of cholesterol efflux to (a) apoAI and (b) HDL was analyzed with the liquid scintillation counting assay. (E) THP-1 cells were differentiated for 72 h with 100 nM PMA and then macrophages were transformed into foam cells by incubation in the presence of 50 μ g/mL of oxidized LDL for 48 h. THP-1 macrophage-derived foam cells were treated with 50 nM miRNA mimics for 48 h, as indicated, and the cholesterol content measured using HPLC. (F) THP-1 cells were differentiated for 72 h with 100 nM PMA and then macrophages were transformed into foam cells by incubation in the presence of 50 μ g/mL of oxidized LDL for 48 h. THP-1 macrophage-derived foam cells were treated with 50 nM miRNA mimics, as indicated, for 48 h, and inflammatory cytokines in the medium measured with ELISA. All results are expressed as mean values \pm S.D. of three independent experiments, each performed in triplicate. * $p<0.05$ vs. control group.

Results

1. Effects of miR-144-3p on ABCA1 expression, cholesterol homeostasis, and inflammation in THP-1 macrophages

ABCA1 is known to play a key role in cholesterol homeostasis and anti-atherosclerosis. Here, we identified a putative miRNA, designated miR-144-3p, which targets human ABCA1, utilizing a combination of TargetScan, miRanda, RNA22, miRDB, miRGen, PITA, EMBL-EBI, starBase, PicTar, RNAhybrid and

miRBase. The sequence and seed pairing of this miRNA are conserved across multiple species. To establish the effect of miR-144-3p on the 3'UTR of human ABCA1, the dual luciferase assay was performed. As shown in Fig. 1A, human ABCA1 mRNA contains two putative complementary sequences to miR-144-3p. Upon co-transfection of 293T cells with wild-type (pMIR-ABCA1-wt) reporter vectors and hsa-miR-144-3p using Lipofectamine 2000 transfection reagent, luciferase activity was significantly decreased. Mutation of binding site 1 or 2 markedly suppressed the

Table 1. Effects of miR-144-3p agomir on plasma lipid and lipoprotein values in apoE^{-/-} mice.

| | Control group (n=10) | Mir-144-3p group (n=10) |
|-----------------|----------------------|-------------------------|
| TG (mmol/L) | 1.41±0.39 | 1.47±0.42 |
| TC (mmol/L) | 27.37±3.35 | 24.13±3.15* |
| HDL-C (mmol/L) | 7.23±1.69 | 5.37±1.59* |
| LDL-C (mmol/L) | 14.32±2.21 | 13.62±2.05 |
| VLDL-C (mmol/L) | 5.82±1.29 | 5.13±1.36 |
| ApoA1 (g/L) | 0.06±0.03 | 0.06±0.02 |
| ApoB (g/L) | 0.16±0.04 | 0.17±0.03 |

Data are expressed as mean ± S.D. The data were compared using the unpaired Student's t-test. * p<0.05 vs. control group.

doi:10.1371/journal.pone.0094997.t001

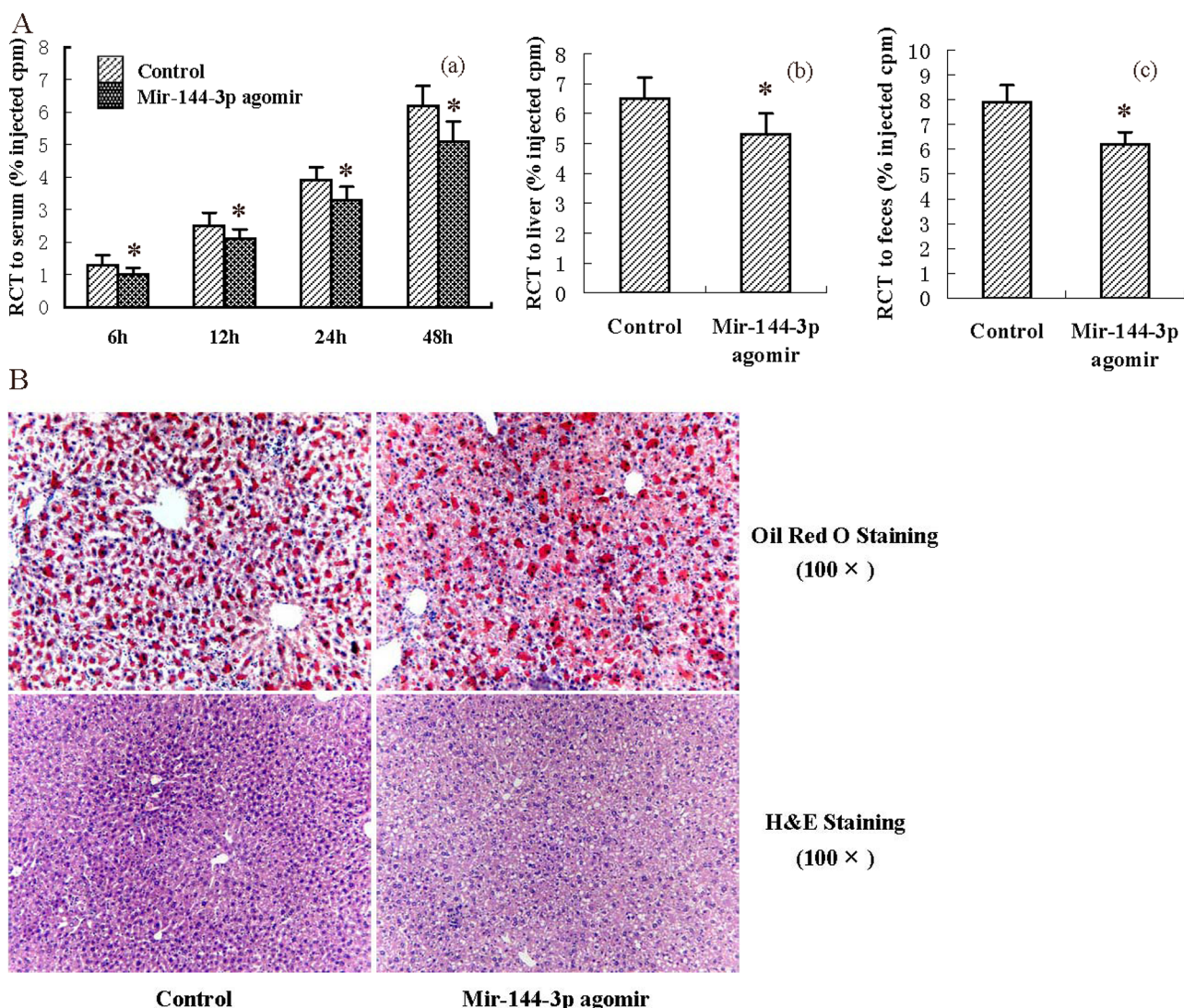


Figure 2. Effects of miR-144-3p on RCT and hepatic lipid deposition. (A) After 12 weeks of the indicated treatment, apoE^{-/-} mice were injected subcutaneously with ³H-cholesterol-labeled, Ac-LDL-loaded bone marrow-derived macrophages. Data are expressed as a percentage of the ³H-cholesterol tracer relative to that of total cpm tracer injected ± S.D.; n=5. * p<0.05 vs. control group. (a) Time-course of ³H-cholesterol distribution in plasma. (b) Hepatic ³H-cholesterol tracer levels after 48 h. (c) Fecal ³H-cholesterol tracer levels. Feces were collected continuously from 0 to 48 h post-injection. (B) Liver cryosections were stained with Oil Red O and hematoxylin. Data are presented as mean values ± S.D.; n=10. * p<0.05 vs. control group.

doi:10.1371/journal.pone.0094997.g002

Table 2. Effects of miR-144-3p agomir on hepatic lipid deposition in apoE^{-/-} mice.

| | Control group (n = 10) | Mir-144-3p group (n = 10) |
|------------------|-------------------------------|----------------------------------|
| TC (mg/g tissue) | 11.56±2.35 | 14.68±2.79* |
| TG (mg/g tissue) | 19.43±2.32 | 20.57±2.16 |

Data are expressed as mean ± S.D. The data were compared using the unpaired Student's t-test. * p<0.05 vs. control group.
doi:10.1371/journal.pone.0094997.t002

effect of hsa-miR-144-3p, while mutation of both binding sites completely reversed the effect of hsa-miR-144-3p.

Macrophages play a central role in atherosclerosis, and ABCA1 is critical for cellular cholesterol efflux. Accordingly, we transfected THP-1 macrophages and human primary macrophages with miR-144-3p mimics or negative control to establish the effect of miR-144-3p on ABCA1 expression. Our results showed that miR-144-3p mimics significantly suppress the ABCA1 mRNA and protein levels in the two cell models (Fig. 1B). Cells transport excess cholesterol across, in part, through the ABCA1 pathway to prevent toxicity resulting from cholesterol overload [16]. To investigate the impact of miR-144-3p on cholesterol homeostasis, cultured THP-1 macrophages were transfected with miR-144-3p mimics. Cholesterol efflux to both apoAI and HDL was markedly decreased, compared to the control group (Fig. 1C). Additionally, total cholesterol, free cholesterol and cholesterol ester levels in THP-1 macrophage-derived foam cells were significantly increased as a result of treatment with miR-144-3p mimics (Fig. 1D).

Atherosclerosis is a complex inflammatory disease, with macrophage foam cells being the major cell type involved in inflammation [17–18]. ABCA1 has been shown to have anti-inflammatory activity independent of its role in RCT. Therefore, we investigated the effects of miR-144-3p mimics on inflammatory factor expression in THP-1 macrophage-derived foam cells. Notably, following treatment with miR-144-3p mimics, secretion of inflammatory cytokines, including TNF-α, IL-1β and IL-6, into culture medium was dramatically increased (Fig. 1E).

2. Effects of miR-144-3p agomir on RCT and inflammation *in vivo*

A combination of genetic and dietary manipulation results in extensive atherosclerotic disease in mice, which has many features in common with human lesions [19]. Since elevated levels of serum cholesterol are probably unique in being sufficient to drive the development of atherosclerosis in humans, we aimed to identify whether miR-144-3p agomir affects the lipid parameters in apoE^{-/-} mice administered HFD. As shown in Table 1, the levels of total cholesterol and HDL-C were markedly decreased in miR-144-3p agomir-treated mice, while changes in apoAI, apoB, LDL-C and VLDL-C concentrations were not statistically significant. Next, we explored the effects of miR-144-3p agomir

on RCT efficiency in experimental mice. As shown, treatment of apoE^{-/-} mice fed a HFD with miR-144-3p agomir resulted in a dramatic decrease in RCT to serum, liver and feces. Interestingly, RCT to serum was downregulated by miR-144-3p agomir in a time-dependent manner (Fig. 2A). HDL mediates reverse transport of cholesterol to the liver for disposal. The liver is proposed to be a metabolic center for lipoproteins and cholesterol. Therefore, we subsequently analyzed the effects of miR-144-3p agomir on morphology and lipid content in the liver of apoE^{-/-} mice with hematoxylin and eosin (H&E) staining and Oil Red O staining, respectively. Representative images of randomly selected sections of liver stained for H&E and Oil Red O in the control and miR-144-3p agomir groups are shown in Fig. 2B. Based on the number of vacuoles and nuclear size, increased lipid deposits in miR-144-3p agomir-treated animals were observed, compared with control animals. Oil Red O staining results additionally disclosed that the miR-144-3p agomir significantly accelerates hepatic lipid deposition in apoE^{-/-} mice. The effects of miR-144-3p agomir on the hepatic lipid content of apoE^{-/-} mice were further measured enzymatically. As shown in Table 2, both hepatic triglyceride and hepatic cholesterol levels in liver were increased in mice treated with miR-144-3p agomir, compared to control mice. We examined the inflammatory cytokine levels *in vivo* with a series of ELISA experiments. Treatment of apoE^{-/-} mice fed a HFD with the miR-144-3p agomir resulted in significant upregulation of plasma TNF-α, IL-1β and IL-6 by 54.3%, 45.6% and 68.4%, respectively (Table 3), consistent with *in vitro* findings. Our data collectively indicate that treatment with miR-144-3p mimics or agomir promotes pro-inflammatory cytokine production, both *in vivo* and *in vitro*.

3. Effect of miR-144-3p agomir on pathological progress of atherosclerosis in apoE^{-/-} mice

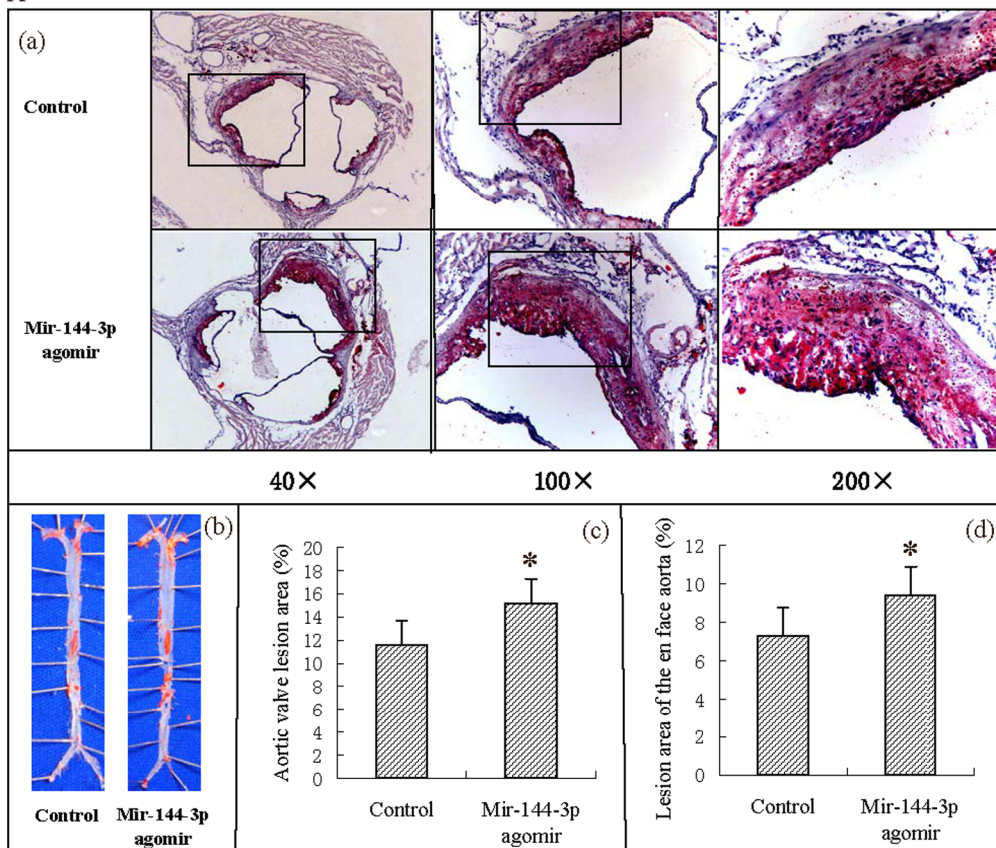
Atherosclerosis is a progressive disease, and clinical events are usually associated with rupture or erosion of the plaque [20]. Accordingly, we investigated the impact of miR-144-3p agomir on atheromatous plaque formation in apoE^{-/-} mice fed HFD. As shown in Fig. 3A, quantification of Oil Red O-stained aortic sinus sections revealed that treatment with miR-144-3p agomir resulted in a significant increase in lesion area (by 30.95%) in apoE^{-/-} mice, compared with control mice. To further establish the

Table 3. Effects of miR-144-3p agomir on plasma cytokine levels in apoE^{-/-} mice.

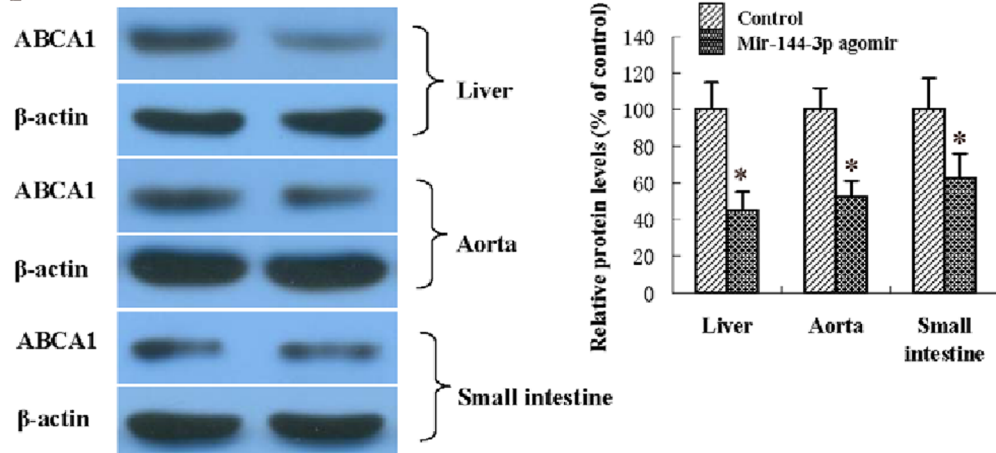
| | Control group (n = 10) | Mir-144-3p group (n = 10) |
|---------------|-------------------------------|----------------------------------|
| IL-1β (pg/mL) | 17.63±3.98 | 25.71±6.69 * |
| IL-6 (pg/mL) | 86.27±9.63 | 145.31±19.66* |
| TNF-α (pg/mL) | 15.26±5.29 | 23.56±7.89* |

Data are expressed as mean ± S.D. The data were compared using the unpaired Student's t-test. * p<0.05 vs. control group.
doi:10.1371/journal.pone.0094997.t003

A



B



C

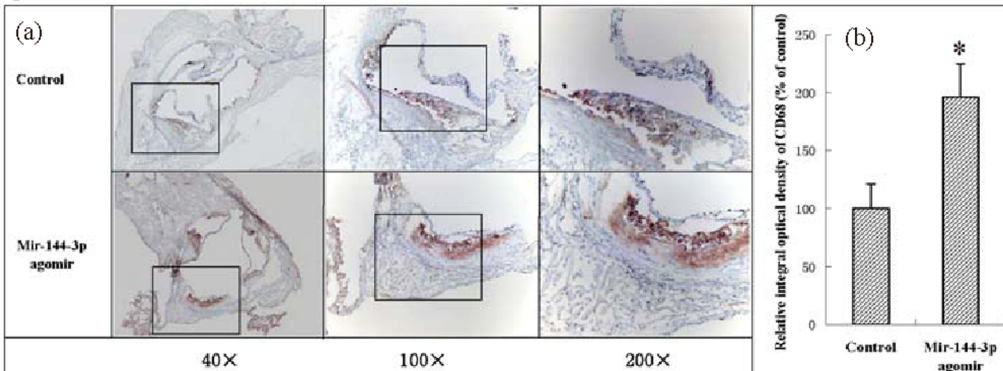


Figure 3. Effects of miR-144-3p on atherosclerosis initiation and development in apoE^{-/-} mice. (A) (a) Representative staining of aortic sinus with Oil Red O. (b) Representative staining of en face aorta with Oil Red O. (c) Lesions in aortic valves were analyzed in apoE^{-/-} mice. (d) En face lesions were analyzed in apoE^{-/-} mice. Data are presented as mean values ± S.D.; n = 10. * p < 0.05 vs. control group. (B) Protein levels in tissues of apoE^{-/-} mice were analyzed using western blot analysis. Data are presented as mean values ± S.D.; n = 5. * p < 0.05 vs. control group. (C) (a) Cryo-sections of aortic valves from apoE^{-/-} mice were immunohistochemically stained for the macrophage marker, CD68. (b) The integral optical density of CD68 in aortic valve cryo-sections from apoE^{-/-} mice was analyzed. Data are presented as mean values ± S.D.; n = 10. * p < 0.05 vs. control group.
doi:10.1371/journal.pone.0094997.g003

negative effects of miR-144-3p agomir on atherosclerosis, Oil Red O-stained lesions in en face preparations of aortas were quantified. Treatment of apoE^{-/-} mice with the miR-144-3p agomir led to a significant increase in lesion area (by 28.77%), compared with control mice. Since liver, small intestine and aorta are the most ABCA1-rich organs, we further explored the effect of miR-144-3p agomir on ABCA1 protein levels in apoE^{-/-} mice. Notably, miR-144-3p agomir downregulated ABCA1 protein expression in liver, aorta and small intestine (Fig. 3B). In addition, we performed immunohistochemical staining to visualize macrophages in atherosclerotic lesions (using an antibody against CD68). As shown, the CD68+ cell number in miR-144-3p agomir-treated mice was significantly increased, compared with that in control mice, indicating markedly higher macrophage infiltration in lesions of apoE^{-/-} mice. These findings clearly indicate a negative effect of miR-144-3p agomir in atherosclerotic lesions of apoE^{-/-} mice.

4. Circulating miR-144-3p is associated with acute myocardial infarction

In view of the finding that miR-144-3p is implicated in atherosclerosis, we investigated the serum miR-144-3p concentrations in 50 subjects. The clinical and biochemical characteristics of these subjects are presented in Table 4. Patients with AMI had significantly higher levels of creatine phosphokinase, creatine phosphokinase-MB fraction, lactate dehydrogenase, aspartate aminotransferase, and alanine aminotransferase. Table 5 shows the univariate associations between serum miR-144-3p concentration and concentrations of other biochemical characteristics. The serum miR-144-3p concentration was negatively correlated with serum HDL levels, and positively correlated with serum glucose concentrations in all subjects. In addition, serum miR-144-3p was positively correlated with serum creatine kinase (CK), creatine kinase-MB fraction (CK-MB), lactate dehydrogenase

Table 4. Clinical characteristics of patients.

| Characteristics | AMI | Healthy outpatient | p Value |
|---|------------|--------------------|---------|
| Age (years) | 63.5±8.6 | 62±7.3 | >0.05 |
| Male/female (n/n) | 15/10 | 17/8 | >0.05 |
| Current smoking, n (%) | 6 (24%) | 5 (20%) | >0.05 |
| Diabetes mellitus, n (%) | 3 (12%) | 2 (8%) | >0.05 |
| Hypertension, n (%) | 12 (48%) | 9 (36%) | >0.05 |
| Hyperlipidaemia, n (%) | 3 (12%) | 1 (4%) | >0.05 |
| Systolic blood pressure (mmHg) | 135±22.3 | 123±19.6 | >0.05 |
| Diastolic blood pressure (mmHg) | 85±15 | 73±14 | >0.05 |
| Glucose (mmol/L) | 6.75±1.63 | 5.90±1.56 | >0.05 |
| Creatine phosphokinase (IU/L) | 1236±453 | 98±11 | 0.0002 |
| Creatine phosphokinase-MB fraction (IU/L) | 86.7±36.5 | 12.5±1.3 | 0.0005 |
| Lactate dehydrogenase (IU/L) | 532±96.2 | 223±16.8 | 0.0312 |
| C-reactive protein (mg/dL) | 1.6±0.5 | 1.0±0.3 | >0.05 |
| Aspartate aminotransferase (IU/L) | 132.6±41.3 | 26.7±6.5 | 0.0006 |
| Alanine aminotransferase (IU/L) | 36.5±7.5 | 23.7±6.8 | 0.0435 |
| Total cholesterol (mmol/L) | 4.23±0.8 | 4.06±0.7 | >0.05 |
| Total triglyceride (mmol/L) | 1.52±1.1 | 1.45±0.8 | >0.05 |
| High-density lipoprotein (mmol/L) | 1.02±0.22 | 1.25±0.39 | >0.05 |
| Low-density lipoprotein (mmol/L) | 2.71±0.67 | 2.46±0.69 | >0.05 |
| ApoA-I (g/L) | 1.23±0.12 | 1.46±0.19 | >0.05 |
| ApoB (g/L) | 1.12±0.28 | 1.06±0.21 | >0.05 |
| Platelets ($\times 10^9$ /L) | 236±35 | 186±28 | >0.05 |
| Creatinine (μ mol/L) | 96±58 | 68±32 | >0.05 |
| Blood urea nitrogen (mg/dL) | 22.3±2.2 | 19.6±1.9 | >0.05 |
| Hemoglobin (g/dL) | 12.6±0.7 | 13.5±0.8 | >0.05 |
| Hemoglobin A1c (%) | 6.2±0.3 | 6.3±0.4 | >0.05 |

AMI indicates acute myocardial infarction; p-value indicates comparison between patients with healthy adults. Data are expressed as mean ± S.D. The data were compared using the unpaired Student's t-test.

doi:10.1371/journal.pone.0094997.t004

Table 5. Associations (Pearson correlation coefficients) of the serum miR-144-3p concentration with biochemical characteristics of subjects.

| | mir-144-3p | | | |
|---|---------------|-------|--------|-------|
| | Healthy adult | | AMI | |
| | r | p | r | p |
| Glucose (mmol/L) | 0.312 | 0.041 | 0.337 | 0.038 |
| Creatine phosphokinase (IU/L) | 0.457 | 0.065 | 0.675 | 0.016 |
| Creatine phosphokinase-MB fraction (IU/L) | 0.556 | 0.081 | 0.625 | 0.033 |
| Lactate dehydrogenase (IU/L) | 0.223 | 0.735 | 0.351 | 0.012 |
| C-reactive protein (mg/dL) | 0.095 | 0.359 | 0.087 | 0.515 |
| Aspartate aminotransferase (IU/L) | 0.331 | 0.069 | 0.416 | 0.046 |
| Alanine aminotransferase (IU/L) | 0.312 | 0.617 | 0.331 | 0.143 |
| Total cholesterol (mmol/L) | 0.219 | 0.446 | 0.167 | 0.548 |
| Total triglyceride (mmol/L) | 0.326 | 0.361 | 0.296 | 0.225 |
| High-density lipoprotein (mmol/L) | -0.217 | 0.008 | -0.316 | 0.009 |
| Low-density lipoprotein (mmol/L) | 0.176 | 0.326 | 0.218 | 0.239 |
| ApoA-I (g/L) | -0.047 | 0.661 | -0.068 | 0.669 |
| ApoB (g/L) | 0.376 | 0.098 | 0.415 | 0.121 |
| Platelets ($\times 10^9$ /L) | 0.213 | 0.663 | 0.562 | 0.356 |
| Creatinine ($\mu\text{mol/L}$) | 0.127 | 0.823 | 0.125 | 0.669 |
| Blood urea nitrogen (mg/dL) | 0.337 | 0.325 | 0.413 | 0.652 |
| Hemoglobin (g/dL) | 0.175 | 0.256 | 0.215 | 0.338 |
| Hemoglobin A1c (%) | 0.326 | 0.078 | 0.412 | 0.083 |

doi:10.1371/journal.pone.0094997.t005

(LDH) and aspartate aminotransferase concentrations in subjects with AMI. We analyzed the expression levels of miR-144-3p in AMI patients after the onset of symptoms and healthy adults at the time-points of 4 h, 8 h, 12 h, 24 h, 48 h, 72 h and 1 week, respectively, as shown in Table 6. Patients with AMI exhibited a 2.16 (± 0.12)-fold, 13.52 (± 3.87)-fold and 4.38 (± 1.53)-fold increase in serum miR-144-3p at 4, 8 and 12 h, respectively. The ROC curve of mir-144-3p revealed a moderate ability to distinguish between the AMI and the healthy control group at 4, 8 and 12 h, with AUC values of 0.81, 0.86, and 0.83, respectively.

Discussion

Atherosclerotic cardiovascular disease remains a major and expensive health burden. A strong independent inverse relationship of plasma HDL levels with atherosclerotic cardiovascular disease has been reported. Although HDL has cardioprotective activity via multiple mechanisms, one major activity is its role in RCT [1–2], which is controlled by ATP-binding cassette transporters, particularly ABCA1[4–5]. The protein level and activity of ABCA1 are modulated via both transcriptional and posttranscriptional processes. Members of a class of miRNAs have been recently identified as potent posttranscriptional regulators of ABCA1 [7–9]. In the present study, we identified a putative miRNA, miR-144-3p, which targets 3'UTRs of human ABCA1 and causes post-transcriptional repression. Our results showed that a miR-144-3p agonist effectively accelerates atheromatous plaque formation in apoE^{-/-} mice by simultaneously impairing RCT and promoting pro-inflammatory cytokine production.

Studies on cultural cells and animal models have shown that treatment of THP-1 macrophage-derived foam cells with miR-144-3p mimics upregulates total cholesterol, free cholesterol and

the cholesterol ester content in cells. Consistently, treatment of apoE^{-/-} mice with miR-144-3p agomir resulted in both impairment of RCT and dramatic decrease in HDL-C in our experiments. Epidemiological and clinical studies have provided considerable evidence that a low level of HDL-C is one of the most important risk factors of atherosclerotic cardiovascular disease (CVD), excess cholesterol in cells is cytotoxic, and accumulation of cholesterol in the artery wall initiates lesions [1,2,21]. HDL is a multifunctional and heterogeneous class of particles that plays an essential physiological role as a vehicle for delivery of peripheral cholesterol to the liver, namely RCT, which is widely believed to account for the inverse relationship between plasma HDL-C level and risk for CVD [22–23]. In addition, HDL exerts a protective effect by inhibiting lipoprotein oxidation, while oxidative modification of HDL impairs its atheroprotective properties and oxidatively modified LDL contributes significantly to intima injury, monocyte recruitment and foam cell formation, all of which are critical events in the initiation and progression of atherosclerosis [24]. The miR-144-3p mimic or agomir induced significant upregulation of different types of cholesterol at the cellular level and downregulated HDL-C in the body, indicating a critical role of miR-144-3p in the complex homeostatic network in cholesterol metabolism. HDL components remove cellular cholesterol via multiple mechanisms involving passive diffusion, interactions with SR-B1, and transport activities of ABCs, in particular, ABCA1 [23,25]. ABCA1 is a cell membrane protein that mediates the transport of cholesterol, phospholipids and other metabolites from cells to lipid-depleted HDL apolipoproteins [26]. This protein is a major determinant of plasma HDL levels and a potent atheroprotective factor [27,28]. In the present study, treatment of THP-1 macrophages with miR-144-3p mimics

Table 6. miR-144-3p [levels] in human AMI patients and healthy adults.

| | AMI (4 h) | AMI (8 h) | AMI (12 h) | AMI (24 h) | AMI (48 h) | AMI (72 h) | AMI (1 w) |
|---------------------------------|------------------|------------------|-------------------|-------------------|-------------------|-------------------|------------------|
| Change fold (vs. Healthy adult) | 2.16±0.12 | 13.52±3.87 | 4.38±1.53 | 1.22±0.15 | 1.17±0.12 | 0.98±0.10 | 1.15±0.13 |
| p-value | 0.015 | 0.001 | 0.008 | | | | |
| AUC | 0.81 | 0.86 | 0.83 | | | | |

Plasma samples were collected at 4 h, 8 h, 12 h, 24 h, 48 h, 72 h and 1 week after the onset of symptoms, and the data expressed as mean values ± S.D. Values indicated a fold change of miR-144-3p level vs. that in the control group. Corresponding p-values were calculated using the independent-samples t-test. Missing p-values represent non-significant miRNA level changes. AUC indicates the area under the receiver operating characteristic (ROC) curve for discrimination between AMI and control groups.
doi:10.1371/journal.pone.0094997.t006

resulted in a marked decrease in cholesterol efflux to both apoAI and HDL. In addition, miR-144-3p agomir suppressed ABCA1 protein expression in liver, aorta and small intestine in apoE^{-/-} mice fed a HFD, and induced a dramatic decrease in RCT to serum, liver and feces. ABCA1 is highly expressed in the liver and tissue macrophages. Liver ABCA1 initiates the formation of HDL particles, while arterial macrophage ABCA1 mediates reverse transport cholesterol and intestinal ABCA1 functions to generate HDL particles that transport dietary cholesterol to the liver. Consequently, decreased ABCA1 expression and activity in organs or tissues would negatively affect the diverse atheroprotective functions of the lipoprotein subclass [29,30]. MiR-144-3p may bind to partially complementary sequences in the 3'UTRs of human ABCA1 and downregulate expression. Moreover, the relative efficiency of the RCT pathway is affected by miR-144-3p mimics or agomir treatment. Although the mechanistic details remain to be defined, this miRNA is proposed to play a critical role in the regulation of cholesterol homeostasis and anti-atherosclerosis.

Accumulating experimental and clinical evidence supports the theory that atherosclerosis is a form of chronic inflammation, and macrophages play a key role. It is widely accepted that recruitment of macrophages and their subsequent foam cells are the major cellular events contributing to the pathological process of atherosclerosis [3]. Recent research has indicated that ABCA1, in addition to lipid transport activity, not only influences inflammatory signaling pathways indirectly by modifying cell surface lipid domains, but also directly acts as an anti-inflammatory receptor by inducing signaling through the Janus kinase 2(JAK2)/STAT3 pathway in response to binding lipid poor apoAI [31,32]. Furthermore, receptors other than ABCA1 that modulate HDL levels and flux of cholesterol through the RCT pathway are reported to have anti-inflammatory properties [33,34]. As a result of miR-144-3p mimic or agomir treatment, expression levels of ABCA1 in cultured cells or experimental mice were remarkably inhibited in our study. Treatment of THP-1 macrophage-derived foam cells with miR-144-3p mimics increased inflammatory cytokine levels, including those of TNF- α , IL-1 β and IL-6. Similarly, the plasma concentrations of TNF- α , IL-1 β and IL-6 in apoE^{-/-} mice fed HFD were dramatically enhanced upon treatment with miR-144-3p agomir. An insight into the pathogenesis of atherosclerosis revealed that uptake of highly oxidized LDL particles by scavenger receptors in macrophages leads to foam cell formation, and expression of scavenger receptors is regulated by cytokines, such as TNF- α and interferon- γ (IFN- γ) [35]. Alternatively TNF- α increases the risk of CAD by interfering with the thrombotic process owing to enhancement of procoagulant activity, and suppresses the antithrombotic protein C pathway in endothelial cells [36]. IL-1 β induces the production of a broad spectrum of cytokines and chemokines, as well as expression of adhesion molecules on endothelial cells, leading to the recruitment of inflammatory cells [37]. Circulating levels of IL-6 represent a strong independent marker of increased mortality among patients with unstable coronary artery disease, and may be useful in directing subsequent care [38]. The miR-144-3p mimic/agomir induced a dramatic increase in the relative levels of types of inflammatory factors levels, both *in vitro* and *in vivo*, confirming its pro-inflammatory property, and therefore, activity as a potent negative regulator of CVD. In addition, treatment of apoE^{-/-} mice with miR-144-3p agomir resulted in increased macrophage infiltration in lesions. As discussed previously, macrophages may initially function as a protective factor, but present a burden to the arterial wall owing to excessive accumulation of ox-LDL. Here, we reported that the miR-144-3p agomir dramatically accelerates the

progress of atheroma in apoE^{-/-} mice by simultaneously increasing the CD68+ cell content in plaque areas and promoting pro-inflammatory cytokine production in plasma.

As plaque rupture and thrombosis convert chronic inflammatory conditions to an acute clinical event and diagnosis with optimal rapidity and sensitivity will benefit both patients and doctors, blood protein markers have been included in the diagnosis or assessment of AMI, including CK-MB, troponin T (TnT) and troponin I (TnI) [39,40]. A clinical investigation by our group revealed that the circulating miR-144-3p concentration is positively correlated with serum CK, CK-MB, LDH and aspartate aminotransferase in AMI subjects. Additionally, the serum miR-144-3p level was elevated within 4 h, reached a peak at 8 h, and was suppressed within 12 h after the onset of chest pain. The ability of miR-144-3p to distinguish between the AMI and control groups was observed from the ROC curves, with AUC values of 0.81, 0.86 and 0.83, respectively. Thus, the plasma concentrations of miR-144-3p showed a significant correlation with those of CK, CK-MB and LDH, a series of classic markers of myocardial injury. Although these markers are robust diagnostic and prognostic indicators in the setting of suspected AMI, there are still perceived limitations [39,41]. Except for rapidity, the ideal nucleotide blood biomarker of AMI should be cardiomyocyte-specific, detectable, and stable in blood. Serum miR-144-3p investigated in the present study corresponds to the above requirements. It is important to note that the current investigation involved a relatively small sample size, and further experimental studies are therefore necessary to explore the underlying mechanisms. Moreover, serum miR-144-3p was negatively correlated with serum HDL and positively correlated with serum glucose concentrations in all subjects. The cardioprotective role of HDL is widely accepted, while high serum glucose is one of the major risk factors of atherosclerosis, and most patients with diabetes die from complications of atherosclerosis [42]. Thus, whether miR-144-3p may contribute to increased risk of cardiovascular disease in diabetics and the underlying mechanism should to be further

investigated. Circulating miRNAs are emerging as novel biomarkers for AMI [43–45]. Huang *et al* showed that lower levels of miR-320b and miR-125b were associated with increased occurrence of AMI [46]. Xiao *et al* demonstrated that serum miR-208a and miR-499 were elevated after AMI and might be potential biomarkers for AMI [47]. Long *et al* found that circulating miR-30a and miR-195 were highly expressed while let-7b was significantly lower in AMI patients at 8 h after onset of AMI and suggested that the plasma concentration of miR-30a, miR-195 and let-7b could be potential indicators for AMI [48]. In the present study, we found that serum miR-144-3p levels were markedly increased in AMI patients after the onset of symptoms and revealed a positive correlation of circulating miR-144-3p with serum CK, CK-MB, LDH and AST in subjects with AMI. These results collectively imply that miR-144-3p plays critical roles in the pathophysiological processes of AMI, and circulating miR-144-3p may serve as a promising biomarker for AMI diagnosis.

Conclusions

Atherosclerosis is not simply an inevitable degenerative consequence of aging, but rather a chronic inflammatory condition. Mir-144-3p targeting ABCA1, the doorkeeper of RCT, resulted in impaired cholesterol efflux and boosted inflammatory response, which effectively accelerated the occurrence and progression of atherosclerosis in apoE^{-/-} mice fed HFD. In conclusion, our study supports the significance of miR-144-3p as a promising therapeutic target for atherosclerosis and potential candidate biomarker of AMI.

Author Contributions

Conceived and designed the experiments: YWH LZ QW. Performed the experiments: YWH YRH SGW JYZ SFL XM YRQ JBL YHS JJG YCW. Analyzed the data: YWH LZ QW. Contributed reagents/materials/analysis tools: YWH YRH. Wrote the paper: YWH YRH SGW. Obtained permission for use of cell line: YWH.

References

- Fisher EA, Feig JE, Hewing B, Hazen SL, Smith JD (2012) High-density lipoprotein function, dysfunction, and reverse cholesterol transport. *Arterioscler Thromb Vasc Biol* 32: 2813–2820.
- Mahdy Ali K, Womnerth A, Huber K, Wojta J (2012) Cardiovascular disease risk reduction by raising HDL cholesterol—current therapies and future opportunities. *Br J Pharmacol* 167: 1177–1194.
- Hansson GK (2009) Atherosclerosis—an immune disease: The Anitschkov Lecture 2007. *Atherosclerosis* 202: 2–10.
- Dean M, Hamon Y, Chimini G (2001) The human ATP-binding cassette (ABC) transporter superfamily. *J Lipid Res* 42: 1007–1017.
- Oram JF, Lawn RM, Garvin MR, Wade DP (2000) ABCA1 is the cAMP-inducible apolipoprotein receptor that mediates cholesterol secretion from macrophages. *J Biol Chem* 275: 34508–34511.
- Brooks-Wilson A, Marcil M, Clee SM, Zhang LH, Roomp K, et al. (1999) Mutations in ABCA1 in Tangier disease and familial high-density lipoprotein deficiency. *Nat Genet* 22: 336–345.
- Rayner KJ, Suárez Y, Dávalos A, Parathath S, Fitzgerald ML, et al. (2010) MiR-33 contributes to the regulation of cholesterol homeostasis. *Science* 328: 1570–1573.
- Najafi-Shoushtari SH, Kristo F, Li Y, Shioda T, Cohen DE, et al. (2010) MicroRNA-33 and the SREBP host genes cooperate to control cholesterol homeostasis. *Science* 328: 1566–1569.
- Sacco J, Adeli K (2012) MicroRNAs: emerging roles in lipid and lipoprotein metabolism. *Curr Opin Lipidol* 23: 220–225.
- Seppen J, Rijnberg M, Cooreman MP, Oude ER (2002) Lentiviral vectors for efficient transduction of isolated primary quiescent hepatocytes. *J Hepatol* 36: 459–465.
- Hu YW, Ma X, Li XX, Liu XH, Xiao J, et al. (2009) Eicosapentaenoic acid reduces ABCA1 serine phosphorylation and impairs ABCA1-dependent cholesterol efflux through cyclic AMP/protein kinase A signaling pathway in THP-1 macrophage-derived foam cells. *Atherosclerosis* 204: e35–43.
- Zhang Y, Da Silva JR, Reilly M, Billheimer JT, Rothblat GH, et al. (2005) Hepatic expression of scavenger receptor class B type I (SR-BI) is a positive regulator of macrophage reverse cholesterol transport in vivo. *J Clin Invest* 115: 2870–4.
- Inoue S, Egashira K, Ni W, Kitamoto S, Usui M, et al. (2002) Anti-monocyte chemoattractant protein-1 gene therapy limits progression and destabilization of established atherosclerosis in apolipoprotein E-knockout mice. *Circulation* 106: 2700–6.
- Recalde HR (1984) A simple method of obtaining monocytes in suspension. *J Immunol Methods* 69: 71–7.
- Morrow DA, Cannon CP, Jesse RL, Newby LK, Ravkilde J, et al. (2007) National Academy of Clinical Biochemistry Laboratory Medicine Practice Guidelines: Clinical characteristics and utilization of biochemical markers in acute coronary syndromes. *Circulation* 115: e356–375.
- Tabas I (2002) Consequences of cellular cholesterol accumulation: basic concepts and physiological implications. *Journal of Clinical Investigation* 110: 905–911.
- Østerud B, Bjorklid E (2003) Role of monocytes in atherogenesis. *Physiological reviews* 83: 1069–1112.
- Libby P, Ridker PM, Maseri A (2002) Inflammation and atherosclerosis. *Circulation* 105: 1135–1143.
- Breslow JL (1996) Mousemodels of atherosclerosis. *Science* 272: 685–688.
- Virmani R, Kolodig FD, Burke AP, Farb A, Schwartz SM (2000) Lessons from sudden coronary death: a comprehensive morphological classification scheme for atherosclerotic lesions. *Arterioscler Thromb Vasc Biol* 20: 1262–1275.
- Guyton JR, Klemp KF (1996) Development of the lipid-rich core in human atherosclerosis. *Arterioscler Thromb Vasc Biol* 16: 4–11.
- Redondo S, Martínez-González J, Urraca C, Tejerina T (2011) merging therapeutic strategies to enhance HDL function. *Lipids Health Dis* 10: 175.
- Barter P (2011) HDL-C: role as a risk modifier. *Atheroscler Suppl* 12: 267–270.
- Watson AD, Leitinger N, Navab M, Faull KF, Höökö S, et al. (1997) Structural identification by mass spectrometry of oxidized phospholipids in minimally oxidized low density lipoprotein that induce monocyte/endothelial interactions and evidence for their presence in vivo. *J Biol Chem* 272: 13597–13607.

25. Farmer JA, Liao J (2011) Evolving concepts of the role of high-density lipoprotein in protection from atherosclerosis. *Curr Atheroscler Rep* 13: 107–114.
26. Oram JF (2003) HDL apolipoproteins and ABCA1 partners in the removal of excess cellular cholesterol. *Arterioscler Thromb Vasc Biol* 23: 720–727.
27. Oram JF, Lawn RM (2011) ABCA1: the gatekeeper for eliminating excess tissue cholesterol. *J Lipid Res* 42: 1173–1179.
28. Wang N, Tall AR (2003) Regulation and mechanisms of ATP-binding cassette transporter A1-mediated cellular cholesterol efflux. *Arterioscler Thromb Vasc Biol* 23: 1178–1184.
29. Wellington CL, Walker EK, Suarez A, Kwok A, Bissada N, et al. (2002) ABCA1 mRNA and protein distribution patterns predict multiple different roles and levels of regulation. *Lab Invest* 82: 273–283.
30. Iqbal J, Anwar K, Hussain MM (2003) Multiple, independently regulated pathways of cholesterol transport across the intestinal epithelial cells. *J Biol Chem* 278: 31610–31620.
31. Yin K, Deng X, Mo ZC, Zhao GJ, Jiang J, et al. (2011) Tristetraprolin-dependent post-transcriptional regulation of inflammatory cytokine mRNA expression by apolipoprotein A-I: role of ATP-binding membrane cassette transporter A1 and signal transducer and activator of transcription 3. *J Biol Chem* 286: 13834–13845.
32. Liu Y, Tang C (2012) Regulation of ABCA1 functions by signaling pathways. *Biochim Biophys Acta* 1821: 522–529.
33. Jahangiri A, de Beer MC, Noffsinger V, Tannock LR, Ramaiah C, et al. (2009) HDL remodeling during the acute phase response. *Arterioscler Thromb Vasc Biol* 29: 261–267.
34. McGillicuddy FC, de la Llera Moya M, Hinkle CC, Joshi MR, Chiquoine EH, et al. (2009) Inflammation impairs reverse cholesterol transport in vivo. *Circulation* 119: 1135–1145.
35. Tontonoz P, Nagy L, Alvarez JG, Thomazy VA, Evans RM (1998) PPARgamma promotes monocyte/macrophage differentiation and uptake of oxidized LDL. *Cell* 93: 241–252.
36. Nawroth PP, Stern DM (1987) Modulation of endothelial cell hemostatic properties by tumor necrosis factor. *Onkologie* 10: 254–258.
37. Dinarello CA (2000) The role of the interleukin-1-receptor antagonist in blocking inflammation mediated by interleukin-1. *N Engl J Med* 343: 732–734.
38. Lindmark E, Diderholm E, Wallentin L, Siegbahn A (2001) Relationship between interleukin 6 and mortality in patients with unstable coronary artery disease. *JAMA* 286: 2107–2113.
39. Bhayana V, Henderson AR (1995) Biochemical markers of myocardial damage. *Clin Biochem* 28: 1–29.
40. Kelley WE, Lockwood CM, Cervelli DR, Sterner J, Scott MG, et al. (2009) Cardiovascular disease testing on the Dimension Vista system: biomarkers of acute coronary syndromes. *Clin Biochem* 42: 1444–1451.
41. Dekker MS, Mosterd A, van 't Hof AW, Hoes AW (2010) Novel biochemical markers in suspected acute coronary syndrome: systematic review and critical appraisal. *Heart* 96: 1001–1010.
42. Beckman JA, Creager MA, Libby P (2002) Diabetes and atherosclerosis: epidemiology, pathophysiology, and management. *JAMA* 287: 2570–2581.
43. Devaux Y, Mueller M, Haaf P, Goretti E, Twerenbold R, et al. (2013) Diagnostic and prognostic value of circulating microRNAs in patients with acute chest pain. *J Intern Med* doi: 10.1111/joim.12183. [Epub ahead of print].
44. Sayed AS, Xia K, Yang TL, Peng J (2013) Circulating microRNAs: a potential role in diagnosis and prognosis of acute myocardial infarction. *Dis Markers* 35: 561–566.
45. Recchioni R, Marcheselli F, Olivieri F, Ricci S, Procopio AD, et al. (2013) Conventional and novel diagnostic biomarkers of acute myocardial infarction: a promising role for circulating microRNAs. *Biomarkers* 18: 547–558.
46. Huang S, Chen M, Li L, He M, Hu D, et al. (2014) Circulating microRNAs and the Occurrence of Acute Myocardial Infarction in Chinese Populations. *Circ Cardiovasc Genet* [Epub ahead of print]
47. Xiao J, Shen B, Li J, Lv D, Zhao Y, et al. (2014) Serum microRNA-499 and microRNA-208a as biomarkers of acute myocardial infarction. *Int J Clin Exp Med* 7: 136–141.
48. Long G, Wang F, Duan Q, Yang S, Chen F, et al. (2012) Circulating miR-30a, miR-195 and let-7b associated with acute myocardial infarction. *PLoS One* 7: e50926.